A Fast Waveguide Port Parameter Extraction Technique for the DGTD Method

Lei Zhao, *Member, IEEE*, Geng Chen, Wenhua Yu, *Senior Member, IEEE*, and Jian-Ming Jin, *Fellow, IEEE*

***Abstract*—A fast waveguide port parameter extraction technique for the discontinuous Galerkin time-domain method is described and investigated for the simulation of waveguide-fed devices. Auxiliary differential equations are employed to handle the convolutions involved in the wave port boundary condition, which results in a significant decrease of the computing cost for implementing the boundary condition at a waveguide port. The accuracy and efficiency of the proposed algorithm are verified by numerical experiments.**

***Index Terms*—Auxiliary differential equations (ADEs), convolution, discontinuous Galerkin time-domain (DGTD) method, waveguide port boundary condition (WPBC).**

I. Introduction

RECENTLY, the development of the discontinuous Galerkin time-domain (DGTD) method for an efficient numerical solution of Maxwell's equations has been a topic of intensive interest [1]–[6]. Compared to the finite-difference time-domain (FDTD) and finite-element (FE) methods, the DGTD possesses most of the FDTD advantages, such as spatially and temporally explicit computation, relatively simple formulation, easy-to-implement parallelization, and linear increase in memory and computational costs with the number of elements, whereas it retains most benefits of the FE method, such as the adaptability to unstructured meshes and spatially high-order convergence. Consequently, the DGTD has attracted significant attention for simulating complex practical problems where the solution may vary drastically and abruptly over the entire domain.

Computation of the scattering parameters of RF, microwave, millimeter-wave, and optical devices is a common task in computational electromagnetics. In general, for the simulation of a waveguide-fed device, it is essential to truncate the computational domain at the wave ports of the device, which should permit to launch desired excitations into the device and absorb all the outgoing waves without nonphysical reflections. A common approach is to use a current sheet to launch a guided wave at an input port and employ a perfectly matched layer (PML) to absorb the outgoing waves at both input and output ports [7], [8]. The use of PML requires a larger computational domain to model the PML region and two auxiliary vector fields to compute the fields inside the PML. A more accurate and efficient wave port modeling is to use a waveguide port boundary condition (WPBC), which has been applied to the FDTD, FE, and DGTD methods [9]–[12]. However, the implementation of the WPBC modeling requires calculating a convolution for each mode included in the WPBC. The computational complexity of this convolution is $O(n^2)$, where n is the total number of time-steps. Thus, the calculation becomes more and more time-consuming as the number of time-steps increases. To overcome this difficulty, an auxiliary differential equation (ADE) was introduced to accelerate the calculation in [12]. However, the efficiency of the ADE-based method was not investigated theoretically and numerically, and the implementation was described briefly only for the Runge–Kutta method for time integration, which is not suitable for problems involving a lossy medium. Potratz *et al.* [13] introduced a method that requires to solve a one-dimenional (1-D) Klein–Gordon equation at each time-step, instead of calculating the convolution directly. This method, however, needs an additional region to be appended behind the wave port, which in turn increases the computing cost.

In this letter, we describe a fast and accurate parameter extraction technique for the DGTD simulation of waveguide-fed devices, in which the WPBC is applied directly to the surface of a wave port and an ADE is then employed to replace the convolution to reduce the computation time. The resultant simulation time and accuracy are investigated by comparing the calculated results with other numerical methods for two examples.

II. Theory and Method

Consider the solution of Maxwell's equations

$$\epsilon\frac{\partial \mathbf{E}}{\partial t} - \nabla \times \mathbf{H} + \mathbf{J} = 0 \quad \mu\frac{\partial \mathbf{H}}{\partial t} + \nabla \times \mathbf{E} = 0 \tag{1}$$

within a general 3-D domain Ω. The computational domain Ω is divided into K elements as $\Omega \approx \bigcup_{k=1}^{K} \Omega_k$. Assume that the approximation solutions to $\mathbf{E}(\mathbf{x}, t)$ and $\mathbf{H}(\mathbf{x}, t)$ can be expressed as a linear combination of basis functions of $\mathbf{\Phi}_i(\mathbf{x})$ [6] inside

Manuscript received June 28, 2017; revised July 21, 2017; accepted August 12, 2017. Date of publication August 15, 2017; date of current version September 25, 2017. This work was supported in part by the National Science Foundation of China under Grant 61372057 and Grant 61671223, and in part by the Open Project of State Key Laboratory of Millimeter Waves under Grant K201613. *(Corresponding author: Lei Zhao.)*

L. Zhao, G. Chen, and W. Yu are with the Center of Computational Science and Engineering, School of Mathematics and Statistics, Jiangsu Normal University, Xuzhou 221100, China (e-mail: leizhao@jsnu.edu.cn; gengchn@163.com; yuwenhua@jsnu.edu.cn).

J.-M. Jin is with the Department of Electrical and Computer Engineering, University of Illinois at Urbana–Champaign, Urbana, IL 61801 USA (e-mail: j-jin1@illinois.edu).

Color versions of one or more of the figures in this letter are available online at http://ieeexplore.ieee.org.

Digital Object Identifier 10.1109/LAWP.2017.2740298

1536-1225 © 2017 IEEE. Personal use is permitted, but republication/redistribution requires IEEE permission.
See http://www.ieee.org/publications_standards/publications/rights/index.html for more information.

element k as

$$\mathbf{E}^k = \sum_{i=1}^{3N_p} E_i^k(t)\mathbf{\Phi}_i(\mathbf{x}) \quad \mathbf{H}^k = \sum_{i=1}^{3N_p} H_i^k(t)\mathbf{\Phi}_i(\mathbf{x}) \tag{2}$$

where $N_p = (p+1)(p+2)(p+3)/6$ is the local number of degrees of freedom associated with the interpolation degree of p, and (E_i^k, H_i^k) denote the nodal values of $(\mathbf{E}^k, \mathbf{H}^k)$. Applying Galerkin's spatial procedure to the resultant equations, we obtain the matrix form for the semidiscretized Maxwell's equations in element k as

$$\epsilon\mathbb{M}\frac{d}{dt}E^k = \mathbb{S}H^k - \sigma_e\mathbb{M}E^k + \kappa_h(\mathbb{F}_1^+H^{k+} - \mathbb{F}_1H^k) - \nu_e(\mathbb{F}_2^+E^{k+} - \mathbb{F}_2E^k) \tag{3}$$

$$\mu\mathbb{M}\frac{d}{dt}H^k = -\mathbb{S}E^k - \kappa_e(\mathbb{F}_1^+E^{k+} - \mathbb{F}_1E^k) - \nu_h(\mathbb{F}_2^+H^{k+} - \mathbb{F}_2H^k) \tag{4}$$

in which κ and ν depend on the electric and magnetic parameters of the materials in element k and all the adjacent elements denoted as $k+$. Using the upwind flux, we have

$$\kappa_e = \frac{Y^{k+}}{Y^k + Y^{k+}} \quad \kappa_h = \frac{Z^{k+}}{Z^k + Z^{k+}} \tag{5}$$

$$\nu_e = \frac{1}{Y^k + Y^{k+}} \quad \nu_h = \frac{1}{Z^k + Z^{k+}}. \tag{6}$$

Also in (3) and (4), $\mathbb{M}$ and $\mathbb{S}$ denote the mass and stiffness matrices, respectively, defined as

$$[\mathbb{M}]_{ij} = \int_{\Omega_k} \mathbf{\Phi}_i \cdot \mathbf{\Phi}_j dv \quad [\mathbb{S}]_{ij} = \int_{\Omega_k} \nabla \times \mathbf{\Phi} \cdot \mathbf{\Phi}_j dv \tag{7}$$

and the flux matrices are defined as

$$[\mathbb{F}_1]_{ij} = \oint_{\partial\Omega_k} (\hat{\mathbf{n}} \times \mathbf{\Phi}_i) \cdot \mathbf{\Phi}_j ds \tag{8}$$

$$[\mathbb{F}_2]_{ij} = \oint_{\partial\Omega_k} (\hat{\mathbf{n}} \times \hat{\mathbf{n}} \times \mathbf{\Phi}_i) \cdot \mathbf{\Phi}_j ds \tag{9}$$

$$[\mathbb{F}_1^+]_{ij} = \oint_{\partial\Omega_k} (\hat{\mathbf{n}} \times \mathbf{\Phi}_i^+) \cdot \mathbf{\Phi}_j ds \tag{10}$$

$$[\mathbb{F}_2^+]_{ij} = \oint_{\partial\Omega_k} (\hat{\mathbf{n}} \times \hat{\mathbf{n}} \times \mathbf{\Phi}_i^+) \cdot \mathbf{\Phi}_j ds. \tag{11}$$

For a homogeneous waveguide made of a perfect electric conductor, the corresponding transverse fields on the wave port S_p can be formulated as follows:

$$\mathbf{E}_{tn}^{\mathrm{TE}}(t) = \frac{d}{dt}f_n^{\mathrm{TE}}(t) \cdot \left(\mu\hat{z} \times \nabla_t\phi_n^{\mathrm{TE}}\right) \tag{12}$$

$$\mathbf{H}_{tn}^{\mathrm{TE}}(t) = \mp\left[\frac{d}{dt}f_n^{\mathrm{TE}}(t) + f_n^{\mathrm{TE}}(t) * h(k_{cn};t)\right] \cdot \nabla_t\phi_n^{\mathrm{TE}} \tag{13}$$

$$\mathbf{E}_{tm}^{\mathrm{TM}}(t) = \mp\left[\frac{d}{dt}f_m^{\mathrm{TM}}(t) + f_m^{\mathrm{TM}}(t) * h(k_{cm};t)\right] \cdot \nabla_t\phi_m^{\mathrm{TM}} \tag{14}$$

$$\mathbf{H}_{tm}^{\mathrm{TM}}(t) = \frac{d}{dt}f_m^{\mathrm{TM}}(t) \cdot \left(-\epsilon\hat{z} \times \nabla_t\phi_m^{\mathrm{TM}}\right) \tag{15}$$

in which

$$f_n^{\mathrm{TE}}(t) = \int_{S_p} H_z(t) \cdot \left(k_{cn}^2\phi_n^{\mathrm{TE}}\right) ds \tag{16}$$

$$f_m^{\mathrm{TM}}(t) = \int_{S_p} E_z(t) \cdot \left(k_{cm}^2\phi_m^{\mathrm{TM}}\right) ds \tag{17}$$

are the modal coefficients of the longitudinal field of modes n and m, respectively, and ϕ_n^{TE} and ϕ_m^{TM} are the eigenfunctions that satisfy the homogeneous Helmholtz equations for TE and TM modes, respectively. The sign * stands for the convolution in the time domain, $h(k_{cm};t)$ and $h(k_{cn};t)$ are the corresponding Laplace transforms of the propagation constants $\gamma_{mz} = \mathrm{j}\sqrt{k_0^2 - k_{cm}^2}$ and $\gamma_{nz} = \mathrm{j}\sqrt{k_0^2 - k_{cn}^2}$ in the frequency domain, and they can be expressed as [14]

$$h(k_c;t) = \frac{k_c}{t}J_1(k_c ct)u(ct) \tag{18}$$

where J_1 denotes the first-order Bessel function, u is the unit-step function, k_c is the cutoff wavenumber, and c is the speed of light in free space.

In the proposed WPBC algorithm, we need to calculate the convolution at each time-step for each mode. It is obvious that the convolution can be written as

$$v(t) = g(t) * h(t) = k_c\int_0^t \frac{g(\tau)}{t-\tau}J_1(k_c c(t-\tau))d\tau \tag{19}$$

where $g(t)$ is the coefficient of the mode. The number of operations in calculating (19) through the whole simulation scales as $n(n+1)$, where n is the total number of time-steps; therefore, the computational complexity of the convolution calculation is $O(n^2)$. To alleviate this drawback, an ADE can be introduced to reduce the computational complexity to $O(n)$. The main idea is to replace (19) with an equivalent differential equation. By using the integral form, the first-order Bessel function $J_1(x)$ can be calculated as

$$J_1(x) = \frac{2x}{\pi}\int_0^{\pi/2} \cos(x\cos\varphi)\sin^2\varphi\, d\varphi. \tag{20}$$

Defining an auxiliary variable

$$w(t,\varphi) = k_c c\int_0^t \frac{\sin[k_c c(t-\tau)\cos\varphi]}{\cos\varphi}g(\tau)\, d\tau \tag{21}$$

we obtain the equivalent form for the convolution in (19) as

$$v(t) = \frac{2}{\pi}\int_0^{\pi/2} \sin^2\varphi\frac{\partial w}{\partial t}d\varphi. \tag{22}$$

Using the fundamental solution $G(a,t) = \sin(at)$ for the differential operator $D(a) = d^2/dt^2 + a^2$, we can rewrite $w(t)$ to its equivalent second-order ordinary differential equation (ODE) as

$$\left[\frac{d^2}{dt^2} + (k_c\cos\varphi)^2\right]w = g(t)k_c^2 c \tag{23}$$

which can be reduced to the first-order ODE system as

$$\frac{dw}{dt} = q(t,\varphi) \quad \frac{dq}{dt} = -(ck_c\cos\varphi)^2 w + g(t)k_c^2 c. \tag{24}$$

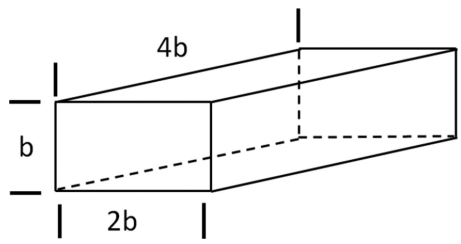

Fig. 1. WR15 rectangular waveguide with $b = 3.76$ mm with both ends truncated with the WPBC.

This equation can be solved by central differencing, and the computed $w(t, \varphi)$ can then be integrated by using trapezoidal integration or Gaussian integration with k quadrature points to obtain $v(t)$. The total number of operations needed are $9kn$, which indicates that the computational complexity of the proposed algorithm is $O(n)$. In general, the ADE system can also be applied to generate the input signal by replacing $g(t)$ with the input signal, which can be a Gaussian pulse, a modulate Gaussian pulse, etc. By using the leap-frog method for time integration, the convolutions in the WPBC for the TE/TM modes can be calculated as

$$g^s = \begin{cases} \int_{S_p} H_z^s \cdot k_c^2 \phi^{\mathrm{TE}} ds, & \text{TE mode} \\ \int_{S_p} E_z^s \cdot k_c^2 \phi^{\mathrm{TM}} ds, & \text{TM mode} \end{cases} \tag{25}$$

$$q^{s+1/2} = q^{s-1/2} - (ck_c \cos\varphi)^2 w^s \Delta t + g^s k_c^2 c \Delta t \tag{26}$$

$$w^{s+1} = w^s + q^{s+1/2} \Delta t \tag{27}$$

$$v^{s+1/2} = \frac{2}{\pi} \int_0^{\pi/2} \sin^2 \varphi \frac{w^{s+1} - w^s}{2} d\varphi. \tag{28}$$

After $v(t)$ is computed, one can use (12)–(15) to obtain the fields on the wave port, which will be assigned as H^+ and E^+ for the numerical fluxes of the DGTD algorithm.

III. Numerical Results

To illustrate the accuracy and efficiency of the proposed ADE-based WPBC implementation in the DGTD method for electromagnetic analysis of waveguide-fed devices, a standard WR15 rectangular waveguide shown in Fig. 1 is considered as the first example. The whole physical model is discretized into 6614 second-order tetrahedral elements. For investigation, the first two guided modes, TE10 and TE01, are launched individually. For each guided mode, the first five modes, TE10, TE01, TE20, TE11, and TM11, are used in the WPBC to truncate the waveguide. The simulation is performed on a laptop with an Intel Core i7-4900MQ@2.8 GHz CPU and an Nvidia GTX 780M GPU card. Fig. 2 shows the results obtained by calculating the convolution $v(t)$ using either the ADE or the direct method, and it is evident that the two results show a good agreement. The time cost for calculating $v(t)$ is also plotted in Fig. 2, which shows an $O(n)$ and $O(n^2)$ complexity for the ADE and the direct convolution methods, respectively. Fig. 3 shows the S-parameters $|S_{11}|$ and $|S_{21}|$ calculated by the ADE method,

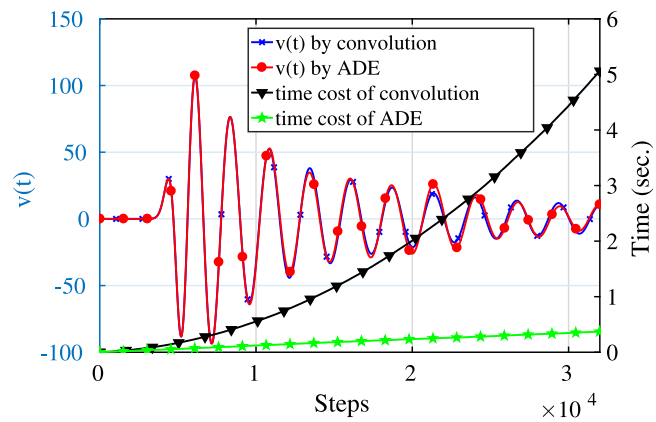

Fig. 2. Numerical computation of $v(t)$ and the associated time cost by the ADE and the direct convolution methods.

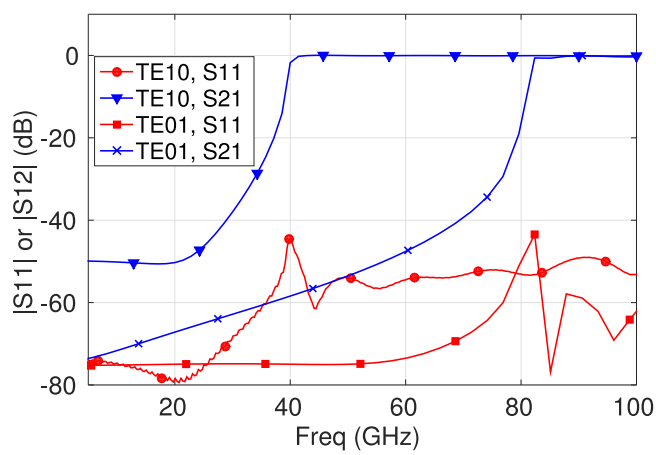

Fig. 3. $|S_{11}|$ and $|S_{21}|$ of the rectangular waveguide for the TE10 and TE01 modes.

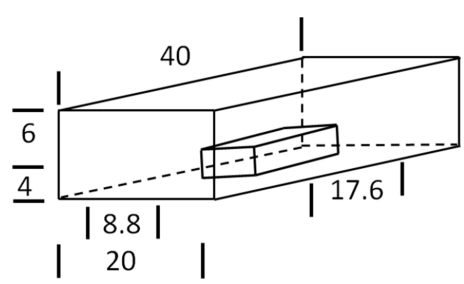

Fig. 4. Dielectric resonator waveguide filter with the relative permittivity of the dielectric block equal to 6.0. Length unit: mm.

which demonstrates a very good performance as the value of $|S_{11}|$ is below -45 dB over the entire frequency range.

To further demonstrate the efficiency and accuracy of the proposed method, a dielectric resonator waveguide filter shown in Fig. 4 with a relative permittivity of 6.0 is simulated. The filter is fed by the TE10 mode, and the first six modes are used in the WPBC applied at the wave ports. The physical model is meshed into 8234 tetrahedral elements. As the dielectric resonator waveguide filter is a highly resonant structure, the simulation requires a very long marching time to obtain converged results. In this

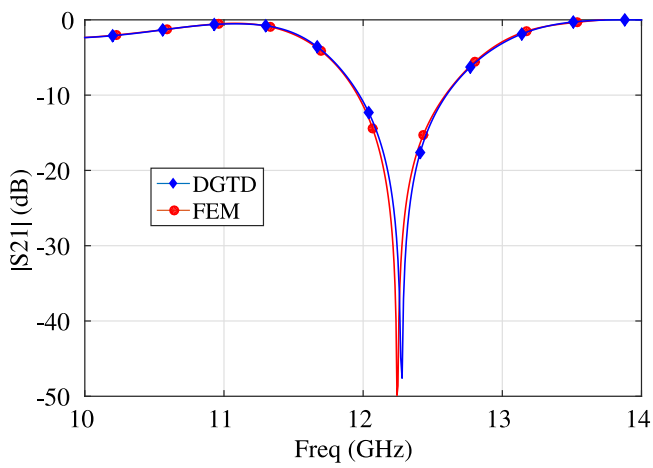

Fig. 5. $|S_{21}|$ of the dielectric resonator waveguide filter computed by the DGTD and FE methods.

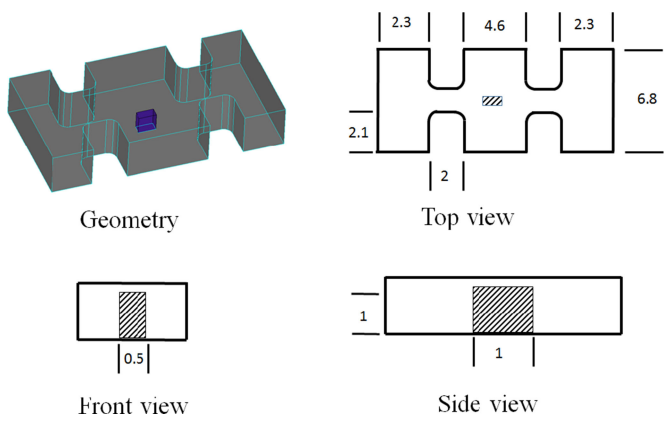

Fig. 6. Configuration of a waveguide filter with a lossy insert. Length unit: mm.

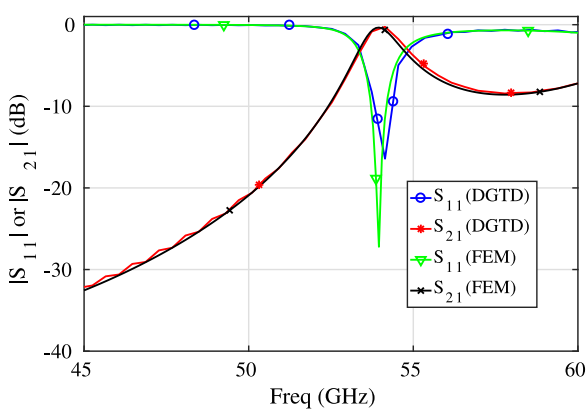

Fig. 7. *S*-parameter of the waveguide filter with a lossy insert.

simulation, the total number of time-steps is 300 239. The computation time cost of the WPBC part using the ADE method is only 5.8 s, whereas the time cost using the direct convolution method is 505 s. Consequently, the total time costs for the simulation with ADE and with direct convolution are 1036 s and 1535 s, respectively, resulting in a reduction in the simulation time by one-third. The computed *S*-parameters are compared with those obtained using the FE method, as shown in Fig. 5, which demonstrates a good agreement.

Finally, a waveguide filter with a lossy insert (with $\epsilon_r = 9$ and $\sigma = 1.0$ S/m) is considered. The configuration and dimensions of the waveguide are demonstrated in Fig. 6. The TE10 mode is used to excite the filter. The calculated *S*-parameters are displayed in Fig. 7, which shows a good agreement between the DGTD results and the ones from the FE method.

IV. Conclusion

In this letter, we described and investigated a fast and accurate wave port parameter extraction method for the DGTD simulation of waveguide-fed devices. Good performance was achieved by using an ADE to speed up the calculation of the convolutions required in the WPBC. The accuracy and efficiency of the proposed algorithm were validated via a standard rectangular waveguide, which has a closed-form solution. The *S*-parameters of a dielectric resonator waveguide filter and a waveguide filter with a lossy insert were simulated with the proposed algorithm, and the results agreed well with those of a commercial software.

References

[1] J. Hesthaven and T. Warburton, *Nodal Discontinuous Galerkin Methods: Algorithms, Analysis, and Applications*. New York, NY, USA: Springer, 2007.

[2] J. Chen and Q. Liu, "Discontinuous Galerkin time-domain methods for multiscale electromagnetic simulations: A review," *Proc. IEEE*, vol. 101, no. 2, pp. 242–254, Feb. 2013.

[3] K. Busch, M. Konig, and J. Niegemann, "Discontinuous Galerkin methods in nanophotonics," *Laser Photon. Rev.*, vol. 5, no. 6, pp. 773–809, 2011.

[4] L. E. Tobon, Q. Ren, Q. Sun, J. Chen, and Q. H. Liu, "New efficient implicit time integration method for DGTD applied to sequential multidomain and multiscale problems," *Prog. Electromagn. Res.*, vol. 151, pp. 1–8, 2015.

[5] L. Zhao, G. Chen, and W. Yu, "GPU accelerated discontinuous Galerkin time domain algorithm for electromagnetic problems of electrically large objects," *Prog. Electromagn. Res. B*, vol. 67, pp. 137–151, 2016.

[6] L. Zhao, G. Chen, and W. Yu, "An efficient algorithm for SAR evaluation from anatomically realistic human head model using DGTD with hybrid meshes," *Appl. Comput. Electromagn. Soc. J.*, vol. 31, no. 6, pp. 629–635, 2016.

[7] Z. J. Cendes and J.-F. Lee, "The transfinite element method for modeling MMIC devices," *IEEE Trans. Microw. Theory Techn.*, vol. 36, no. 12, pp. 1639–1649, Dec. 1988.

[8] X. Ji, T. Lu, W. Cai, and P. Zhang, "Discontinuous Galerkin time domain (DGTD) methods for the study of 2-D waveguide-coupled microring resonators," *J. Lightw. Technol.*, vol. 23, no. 11, pp. 3864–3874, Nov. 2005.

[9] F. Alimenti, P. Mezzanotte, L. Roselli, and R. Sorrentino, "Modal absorption in the FDTD method: A critical review," *Int. J. Numer. Model.*, vol. 10, no. 4, pp. 245–264, 1997.

[10] T.-H. Loh and C. Mias, "Implementation of an exact modal absorbing boundary termination condition for the application of the finite-element time-domain technique to discontinuity problems in closed homogeneous waveguides," *IEEE Trans. Microw. Theory Techn.*, vol. 52, no. 3, pp. 882–888, Mar. 2004.

[11] Z. Lou and J.-M. Jin, "An accurate waveguide port boundary condition for the time-domain finite-element method," *IEEE Trans. Microw. Theory Techn.*, vol. 53, no. 9, pp. 3014–3023, Sep. 2005.

[12] C.-P. Chang, G. Chen, S. Yan, and J.-M. Jin, "Waveport modeling for the DGTD simulation of electromagnetic devices," *Int. J. Numer. Model., Electron. Netw., Devices and Fields*, 2017, doi: 10.1002/jnm.2226.

[13] C. Potratz, H.-W. Glock, and U. van Rienen, "Time-domain field and scattering parameter computation in waveguide structures by GPU accelerated discontinuous-Galerkin method," *IEEE Trans. Microw. Theory Techn.*, vol. 59, no. 11, pp. 2788–2797, Nov. 2011.

[14] J.-M. Jin, *The Finite Element Method in Electromagnetics*, 3rd ed. New York, NY, USA: Wiley, 2015.